



HAL
open science

Magnetic Properties of Two-dimensional Nanodots: Ground State and Phase Transition

Maciej Kasperski, H. Puzzkarski, Danh-Tai Hoang, Hung T. Diep

► **To cite this version:**

Maciej Kasperski, H. Puzzkarski, Danh-Tai Hoang, Hung T. Diep. Magnetic Properties of Two-dimensional Nanodots: Ground State and Phase Transition. 2013. hal-00867361

HAL Id: hal-00867361

<https://hal.science/hal-00867361>

Preprint submitted on 29 Sep 2013

HAL is a multi-disciplinary open access archive for the deposit and dissemination of scientific research documents, whether they are published or not. The documents may come from teaching and research institutions in France or abroad, or from public or private research centers.

L'archive ouverte pluridisciplinaire **HAL**, est destinée au dépôt et à la diffusion de documents scientifiques de niveau recherche, publiés ou non, émanant des établissements d'enseignement et de recherche français ou étrangers, des laboratoires publics ou privés.

Magnetic Properties of Two-dimensional Nanodots: Ground State and Phase Transition

Maciej Kasperski, Henryk Puszkarski

Surface Physics Division, Faculty of Physics, Adam Mickiewicz University, ul. Umultowska 85, 61-614 Poznan, Poland

Danh-Tai Hoang

*Asia Pacific Center for Theoretical Physics, POSTECH, San 31,
Hyoja-dong, Nam-gu, Pohang, Gyeongbuk 790-784, Korea*

H. T. Diep

*Laboratoire de Physique Théorique et Modélisation,
Université de Cergy-Pontoise, CNRS, UMR 8089 2,
Avenue Adolphe Chauvin, F-95302 Cergy-Pontoise Cedex, France*

(Dated: September 29, 2013)

We study the effect of perpendicular single-ion anisotropy, $-As_z^2$, on the ground-state structure and finite-temperature properties of a two-dimensional magnetic nanodot in presence of a dipolar interaction of strength D . By a simulated annealing Monte Carlo method, we show that in the ground state a vortex core perpendicular to the nanodot plane emerges already in the range of moderate anisotropy values above a certain threshold level. In the giant-anisotropy regime the vortex structure is superseded by a stripe domain structure with stripes of alternate domains perpendicular to the surface of the sample. We have also observed an intermediate stage between the vortex and stripe structures, with satellite regions of tilted nonzero perpendicular magnetization around the core. At finite temperatures, at small A , we show by Monte Carlo simulations that there is a transition from the in-plane vortex phase to the disordered phase characterized by a peak in the specific heat and the vanishing vortex order parameter. At stronger A , we observe a discontinuous transition with a large latent heat from the in-plane vortex phase to perpendicular stripe ordering phase before a total disordering at higher temperatures. In the regime of perpendicular stripe domains, namely with giant A , there is no phase transition at finite T : the stripe domains are progressively disordered with increasing T . Finite-size effects are shown and discussed.

PACS numbers: 75.10.-b ; 75.40.Mg ; 85.35.-p ; 85.70.Kh

I. INTRODUCTION

The ground-state (GS) structure of a magnetic nanosystem results from the competition between the interactions in the system. The energies of the exchange and dipolar interactions as well as the anisotropy energy and the energy of interaction of the magnetic moments with the external magnetic field must be taken into account in the energy balance while determining the GS. The combination of the frustration¹ resulting from competing interactions and the boundary effects in nanoscale systems gives rise to unexpected phenomena². Among the competing forces in two dimensions (2D), let us focus on the dipolar interaction which favors in-plane spin configuration, and the perpendicular anisotropy which tends to align spins in the perpendicular axis. The perpendicular anisotropy is known to arise with a large magnitude in ultrathin films^{3,4}. Note that, in thin films with Heisenberg and Potts models, the competing dipolar interaction and perpendicular anisotropy causes a spin re-orientation transition at a finite temperature^{5,6}.

In this paper, we focus on the case of a ultrasmall magnetic nanodot with Heisenberg spins. Four GS configurations have been observed in such nanosystems⁷: (i) a capacitor-like state, (ii) a planar vortex, (iii) a vortex

with core, and (iv) a domain structure. The conditions of formation of each structure have been determined⁷ with the size of the sample, the relation between the exchange and dipolar interactions, and the type of crystal order taken into account. Systems in which the core vortex structure occurs hold much promise from the commercial point of view; the occurrence of this structure has already been demonstrated experimentally⁸⁻¹⁰ by different imaging techniques. A major advantage of core vortex structures is the central region (core) of nonzero perpendicular magnetization, the polarization of which is stable at room temperature (as shown by Shinjo *et al.*⁸). Interestingly, core magnetization reversal^{11,12} can be realized in two ways, by applying a strong magnetic field *perpendicular* to the surface of the sample, or a short pulse of magnetic field *parallel* to it. This property of magnetic nanodots opens the door to their application in magnetoresistive random access memory (MRAM).

The current development of a technology that allows to obtain nanosamples with a very strong perpendicular anisotropy¹³⁻¹⁵ has inspired us to investigate, with the use of Monte Carlo (MC) simulations^{16,17}, the behavior of the core vortex structure, so interesting from the point of view of applications, under the impact of *giant* perpendicular anisotropy.

The purpose of this work is (i) to investigate the GS

configuration in magnetic nanodots taking into account the short-range exchange interaction, the long-range dipolar interaction and the perpendicular anisotropy in 2D, (ii) to study the nature of the ordering and the phase transition at finite temperatures in such nanodots. The methods we employ in this paper are MC simulations with different techniques.

Section II is devoted to the determination of the GS, while section III shows MC results of finite-temperature behaviors. Concluding remarks are given in section IV.

II. GROUND STATE

A. Model and method of ground-state determination

Let us consider a 2D system of Heisenberg spins occupying the sites of a square lattice within a finite $L \times L$ square. The Hamiltonian of the system is assumed to have the standard form:

$$H = -J \sum_{ij}^{\text{nn}} \vec{s}_i \cdot \vec{s}_j - A \sum_i^{\text{all}} (s_i^z)^2 - D \sum_{ij}^{\text{all}} \left[\frac{3(\vec{s}_i \cdot \vec{r}_{ij})(\vec{s}_j \cdot \vec{r}_{ij})}{r_{ij}^5} - \frac{\vec{s}_i \cdot \vec{s}_j}{r_{ij}^3} \right], \quad (1)$$

where J denotes the exchange integral, D is the dipolar coupling parameter, A is the single-ion uniaxial perpendicular anisotropy parameter, \vec{s}_i ($|\vec{s}_i| = 1$ for all i) is the spin at the i -th site, and \vec{r}_{ij} ($r_{ij} = |\vec{r}_{ij}|$) is the position vector connecting the spins at the i -th and j -th sites. The first summation runs over all the nearest-neighbor spin pairs ij , the second one over all the spins in the system, and the third one over all spin pairs. The dipolar energy is calculated from the expression included in the Hamiltonian (1) without any numerical approximations; in particular we do not introduce the cut-off radius, since this has been shown^{7,18} to affect quantitatively the calculation results in a sensible manner. In the following, J is taken as a fixed parameter and is used as the energy unit ($J = 1$). The GS and thermal properties are calculated with varying A and D .

To find the GS of the system defined above we have used the simulated annealing method of the MC simulation class¹⁷. The main steps of the procedure are:

(i) to generate a random spin configuration, which corresponds to a high temperature phase of the system,

(ii) to update one by one all the spins as follows. At a lattice site we calculate the energy of its spin E_1 . Then, we take a random spin orientation and calculate its new energy E_2 . If $E_2 < E_1$ the new spin orientation is accepted. Otherwise, it is accepted only with a probability $p = \exp[-(E_2 - E_1)/k_B T]$ where k_B is the Boltzmann constant and T temperature,

(iii) to repeat the previous step a sufficient number of times,

(iv) to reduce the temperature T and get back to step (ii). With decreasing temperature, the spins converge closer and closer to the GS with iterations.

The above algorithm is thus a ‘‘slow cooling’’ procedure which works rather well for small systems without strong bond disorder. Another way to get the GS is to use the steepest-descent method: i) we generate an initial spin configuration, ii) at each lattice site we calculate the local field from other spins acting on that site, iii) we align the spin of that site along the local field to minimize its energy, iv) we take another spin and repeat step ii) until all spins are considered, iv) we iterate the procedure a large number of times until the convergence of the system energy to a minimum. In general, except for spin glasses, systems without strong bond disorder converges to the GS with a few dozens to a few hundred iterations²⁰. We have checked that this method gives the same results as those obtained from the simulated annealing shown in the following.

B. Evolution of the ground state: formation of the vortex core and stripe domains

To investigate the evolution of the GS with growing anisotropy let us first consider the case shown in Fig. 1, with $L = 10$ and the other parameters fixed at $J = 1$ and $D = 0.3$. The colors indicate the spin orientations: green for in-plane, blue for down, and red for up spins. When the anisotropy is small, the GS is seen to be a planar vortex state, with all the spins lying in the plane of the system. However, above a certain threshold anisotropy value (in this case $A = 0.75$) the spins begin to draw forward from the plane of the system in its central region, which we shall refer to as the vortex core; both magnetization directions - upward and downward - are energetically equivalent. As A continues to grow, above a second threshold value (of 1.57) the minimum energy configuration becomes a stripe structure with alternating stripes of upward and downward spins perpendicular to the plane of the system. (It is noteworthy that the threshold value of 0.75 for which the core has emerged in our study is very close to that calculated analytically²¹ and numerically²² for a spin system of similar size, but only with the exchange interaction.)

Now, let us scrutinize the evolution, shown in Fig. 2, of the GS of the system with much stronger dipolar interaction ($J = 1$, $D = 0.5$). The nonzero magnetization regions are seen to start forming at the corners rather than in the center of the sample (the threshold value of A is 1.32); only above a second threshold value, $A = 1.47$, does the core emerge. The next configuration, which occurs for A greater than 1.87, is characterized by satellite regions of perpendicular magnetization around the core; the magnetization polarization in these regions is opposite to that in the core. Finally, in its further evolution the system achieves a stripe domain structure, which forms above another threshold value, 2.37, of the

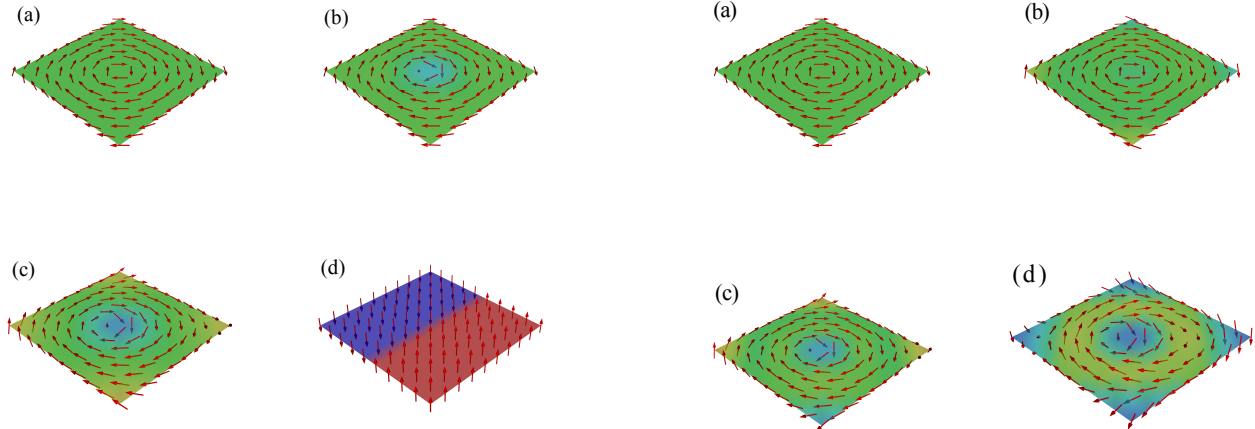


Figure 1. (Color online) Ground state structures established for the below-specified ranges of perpendicular anisotropy (parameter A), with the following values of the other parameters assumed: nanodot size $L = 10$, exchange integral $J = 1$ and dipolar coupling $D = 0.3$. The colors indicate the orientation of spins: green for in-plane spins, blue for down spins and red for up spins. The intensity of each color expresses the degree of spin aligning: (a) planar vortex $0 < A < 0.75$, (b) vortex with core $0.75 < A < 0.95$, (c) vortex with core and corners $0.95 < A < 1.57$, (d) domain structure (stripes) $A > 1.57$.

anisotropy parameter A .

C. Stripe structures

Thus, our simulations indicate that the stripe structure is the final configuration which the spin system seeks in the giant perpendicular anisotropy regime. This finding is easy to accept as with such a strong anisotropy all the spins are drawn out of the sample plane to set along its normal, i.e. $\vec{s}_i = (0, 0, \pm 1)$ for all i . Then the Hamiltonian (1) takes the form:

$$H = -J \sum_{ij}^{\text{nn}} s_i^z s_j^z + D \sum_{ij}^{\text{all}} \frac{s_i^z s_j^z}{r_{ij}^3} - AL^2, \quad (2)$$

which implies that the anisotropy term only shifts the system energy level; for this very reason the number of stripe domains (and their pattern) at a given GS proves to depend only on the ratio D/J , and not on A . Referring to the Hamiltonian (2), we can precisely indicate the ranges in which the stripe structure minimizes the system energy. The results of our investigations are shown in Fig. 3, presenting the evolution of the stripe system with growing D/J ratio. In the figure caption, we specify the stability ranges for each of the depicted stripe structures. The way in which these ranges have been determined is made clear in Fig. 4, which allows to compare the total

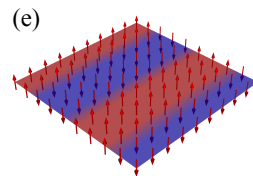


Figure 2. (Color online) Ground state structures established for the below-specified ranges of perpendicular anisotropy (parameter A), with the following values of the other parameters assumed: nanodot size $L = 10$, exchange integral $J = 1$ and dipolar coupling $D = 0.5$. The same color codes as in Fig. 1 are used: (a) planar vortex $0 < A < 1.32$, (b) vortex with corners $1.32 < A < 1.47$, (c) vortex with core and corners $1.47 < A < 1.87$, (d) satellite formation $1.87 < A < 2.37$, (e) domain structure (stripes) $A > 2.37$.

energy of the considered stripe structures (for a specific D/J ratio) to find the lowest-energy structure.

Let us briefly summarize and give a qualitative explanation on the GS's found above. For very low A , the dipolar term dominates, yielding an in-plane vortex configuration. For larger A , spins are ordered in vortex configurations with out-of-plane core and corner spins which is a compromise between D and A effects. For very large A , the energy is lowest when spins are perpendicular. In this situation, the effects of J and D come to determine whether they should be up or down or both: J favors parallel neighbors while D favors antiparallel spins, as seen by examining the signs of these terms in Eq. (2). Increasing D will thus favor antiparallel “domains”. Therefore, the larger D becomes the more numerous domains are created, as we observe in Fig. 3.

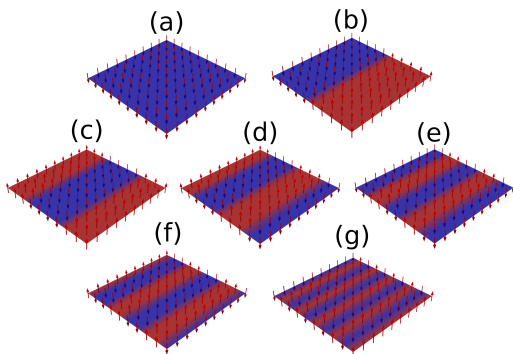


Figure 3. (Color online) Stripe domain ground-state structures established for different values of the D/J in the giant perpendicular anisotropy regime: (a) $D/J=0.00-0.25$, (b) $D/J=0.25-0.32$, (c) $D/J=0.32-0.40$, (d) $D/J=0.40-0.50$, (e) $D/J=0.50-0.58$, (f) $D/J=0.58-0.83$, (g) $D/J=0.83-4$. Simulations were performed for $L = 10$, $J = 1$ and $A = 4$. The same color codes as in Fig. 1 are used.

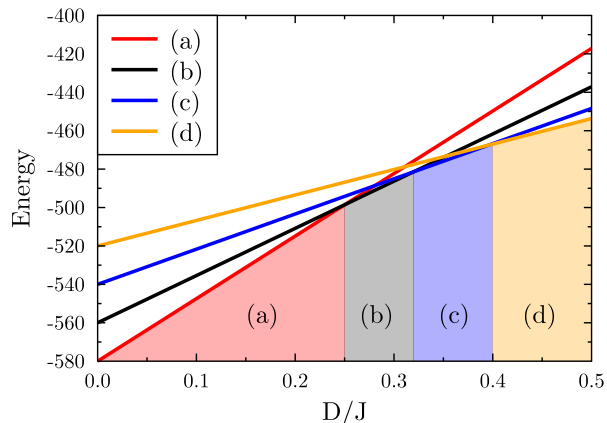


Figure 4. (Color online) Total energy (computed from Eq. (2)) of the spin structures shown in Fig. 3 vs. D/J . These plots provide a basis for determining the minimum-energy structure for a given value of D/J .

III. FINITE-TEMPERATURE PROPERTIES

In statistical physics, a phase transition is defined for systems at the thermodynamic limit where thermodynamic functions diverge or undergo anomalies. Two often encountered types of phase transition are (i) the second-order transition where the second derivatives of the free energy, such as the specific heat and the susceptibility, diverge at the infinite system size, (ii) the first-order transition where the first derivatives of the free energy, such as the internal energy and the magnetization, have discontinuity. We cannot theoretically define a phase transition for a finite-size system. In simulations and in theories, we can study finite-size systems but we use the finite-size scaling^{16,23,24} to predict the characteristics of the phase transition at the infinite-size limit. In nanodots with short-range interaction for instance, we cannot talk

about phase transition in the sense of the above definition: due to their very small sizes, the spins spend a finite time to reverse their orientation over and over again during the simulation time so that there is no stabilized ordering. However, in systems with long-range interaction where each spin is in interaction with all others as the dipolar case treated here, the ground-state ordering is due to the whole all-spin connection: exciting a spin costs an important energy amount, unlike in the short-range interaction case. As it turns out, the GS found above is stabilized at finite temperatures and is destroyed only at a higher temperature. We shall use the term “transition” to indicate this change of ordering which is seen by the variation of the order parameter, even if this transition does not occur with a divergence of physical quantities since we work with nanodots. The dependence of physical quantities on the system size in the transition temperature region proves that the anomaly is indeed a phase transition if we let the system size go to infinity. We will return to this point below.

A second point which is important to emphasize is the following. We know from the Mermin-Wagner theorem²⁵ that systems of spins of continuous degrees of freedom, such as XY or Heisenberg spins, with isotropic short-range interactions do not have long-range ordering at finite T in 2D. Our present model, though having a very small size, possesses the long-range interaction and an Ising-like anisotropy, namely the two factors which favor the ordering at finite T . We will see below that we have, even in the most unfavorable case with small A , a sharp peak of the specific heat at the loss of vortex ordering at a finite T .

We use the standard MC simulation method which is enough for our purpose. The histogram method is used to detect first-order transition when necessary. In general, we discard about 10^6 MC steps per spin for equilibrating and average physical quantities over the next $N_{MC} = 10^6$ MC steps per spin. We will concentrate ourselves in the following to the case $D = 0.3$ with varying A , for numerical presentation. Note however that physical behaviors depend roughly on the ratio A/D .

Let us define the following order parameters depending on the phase symmetry:

- (i) In-plane vortex phase:

$$M_v = \frac{1}{N \times N_{MC}} \times \sum_{t=1}^{N_{MC}} \left| \left[\sum_i^{\text{all}} [\vec{u}_i \wedge \vec{s}_i(t)] / \sin a_0 \right]_z \right| \quad (3)$$

where $N = L^2$, $\vec{u}_i = \vec{r}_i/r_i$ (unit vector along the vector \vec{r}_i connecting the center of the dot and the lattice site i), a_0 is the angle between the spin \vec{s}_i and \vec{u}_i in the GS. Note that M_v is used only when the GS is not ferromagnetic. At $T = 0$, if the configuration is planar, we have $[\vec{u}_i \wedge \vec{s}_i / \sin a_0]_z = 1$ for any i , so that $M_v = 1$. If the configuration is perpendicular, $[\vec{u}_i \wedge \vec{s}_i]_z = 0$ for any i ,

so that $M_v = 0$. When the system is disordered $M_v = 0$ because $\vec{u}_i \wedge \vec{s}_i(t)$ is a random vector. In the vortex GS configuration with core, spins at the dot center are not in the xy plane, so the value of $[\vec{u}_i \wedge \vec{s}_i]_z$ is between 0 (if perpendicular) and $q < 1$ (if tilted). Hence M_v is not saturated at 1 in the GS as seen below.

(ii) Uniform perpendicular configuration:

$$M_z = \frac{1}{N \times N_{MC}} \sum_{t=1}^{N_{MC}} \left| \sum_i^{\text{all}} s_i^z(t) \right| \quad (4)$$

(iii) Stripe configuration:

$$M_s = \frac{1}{N \times N_{MC}} \sum_{t=1}^{N_{MC}} \left| \sum_i^{\text{all}} (-1)^p s_i^z(t) \right| \quad (5)$$

where p is the “parity” of the z domain ($p = \pm 1$ for GS down and up domains respectively).

In the case of weak anisotropy, the dipolar interaction yields an in-plane vortex configuration without core, as seen above. As T increases, we observe a sharp transition from the vortex configuration to the disordered phase, as shown in Fig. 5, for $A/D = 2$. The same behavior is seen for $A/D = 0$ to $\simeq 3$ for $L = 10$. When the dot size is increased, the dipolar contribution to the energy is larger, so the overall energy is more important as seen in the figure at low T , making the transition temperature higher. Note that the peak of the specific heat C_v is very sensitive to the system size, indicating that it corresponds to a real phase transition. The same effect is seen in the order parameter M_v shown in Fig. 5: increasing L makes the fall of M_v much sharper at the transition temperature, namely a higher peak of the susceptibility (not shown). It is interesting to study systematically many larger sizes and to use the finite-size scaling^{16,23,24,26,27} to determine the type of the transition, namely its universality class. Such a formidable task is out of the scope of this paper, it is left for a future investigation.

For larger anisotropies, there is a first-order transition at low T as seen in Fig. 6 with $A/D = 1.4/0.3 \simeq 4.6$: this transition occurring at $T \simeq 0.1$ changes the system ordering from the vortex configuration with core to the perpendicular stripe configuration. The energy undergoes a large discontinuity at the transition. It is interesting to note that the vortex core at $T = 0$ is characterized by a non zero M_z and a non saturated in-plane order parameter M_v . M_z decreases when T is increased from 0. At the transition from the in-plane vortex to the perpendicular stripe configuration M_s jumps to a high value while M_v goes down to 0. When T is increased further, the perpendicular stripe configuration becomes progressively disordered. The system is entirely disordered for $T > 0.45$ for $L = 10$. This is not a phase transition because the peak of C_v does not depend on L as seen in Fig. 6.

We show in Fig. 7 snapshots of the dot at three typical temperature regions: $T = 0.01$ below the transition, $T = 0.19$ in the perpendicular configuration, and $T = 0.82$ in

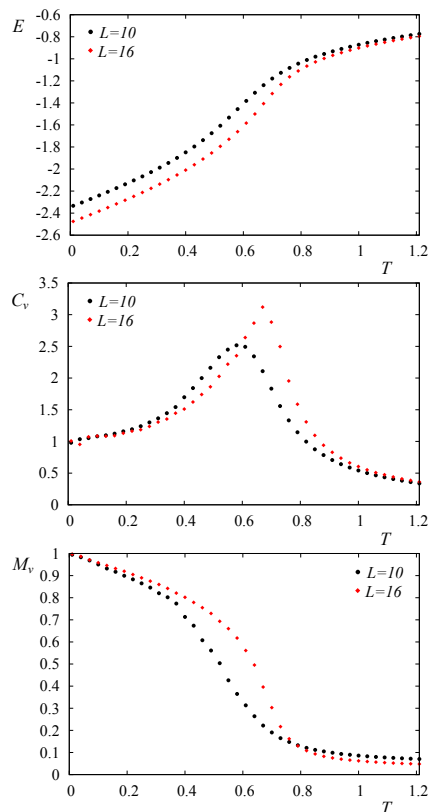


Figure 5. (Color online) Top: Energy per spin, Middle: Specific heat, Bottom: In-plane vortex order parameter M_v , versus T for $A/D = 2$ with $L = 10$ (black circles) and $L = 16$ (red diamonds).

the disordered state. We clearly see that the snapshot at $T = 0.01$ shows the out-of-plane vortex at the core and at the corners.

The first-order transition is confirmed by the double peak structure in the energy histogram taken at the transition temperature $T_c = 0.111$ shown in Fig. 8: the distance between the two peaks indicates a latent heat.

For very large anisotropies, namely for the GS stripe domains, there is no more phase transition as seen in Fig. 9 where the peak of C_v is constant with varying system size. We emphasize here that when the spins are perpendicular to the plane, the first dipolar term in Eq. (1) is zero (because $\vec{s}_i \cdot \vec{r}_{ij} = 0$), and the second dipolar sum is very small due to the compensation of positive and negative energies of parallel and antiparallel spins in the sum. Therefore, for a larger dot size, we have a larger dipolar sum but it does not change the energy per spin as seen in Fig. 9, unlike in the case of in-plane configuration shown in Fig. 5 where the energy is lowered with increasing L , resulting in a higher value of T_c .

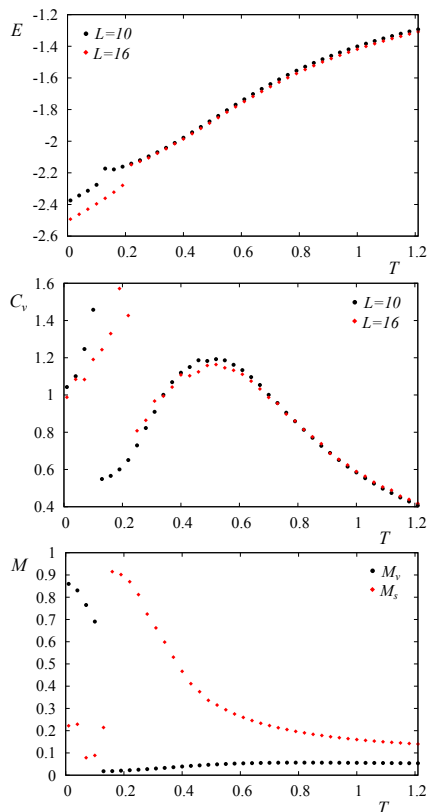


Figure 6. (Color online) Top: Energy, Middle: Specific heat, Bottom: In-plane order parameter M_v and perpendicular stripe magnetization M_s , versus T , for $A/D = 1.4/0.3 \simeq 4.6$, with $L = 10$ (black circles) and $L = 16$ (red diamonds).

IV. CONCLUSION

We have used the simulated annealing MC method for investigating the effect of the perpendicular anisotropy on the ground-state structure of a 2D spin nanodot in the presence of a dipolar interaction. A core, or region of nonzero magnetization perpendicular to the plane of the system, has been demonstrated to form in the considered nanodot only above a certain threshold value of anisotropy A , and this threshold value to grow with the ratio between D , the dipolar coupling, and J the exchange integral. It also depends on the linear size L of the sample due to the long-range dipolar interaction. In addition, we have observed that with increasing A the regions of nonzero perpendicular magnetization first emerge at the corners of the sample and only afterwards in the center. For very large values of D the GS takes the form of a stripe domain structure; we have analyzed thoroughly the impact of the parameters A , J and D on this domain structure. The stripe pattern, namely the number of opposite domains, is shown to depend only on the D/J ratio and to be independent of A in the "perpendicular" regime, namely regime permitted by large enough A . This allowed the assignment of each stripe structure to the corresponding range of D/J as shown

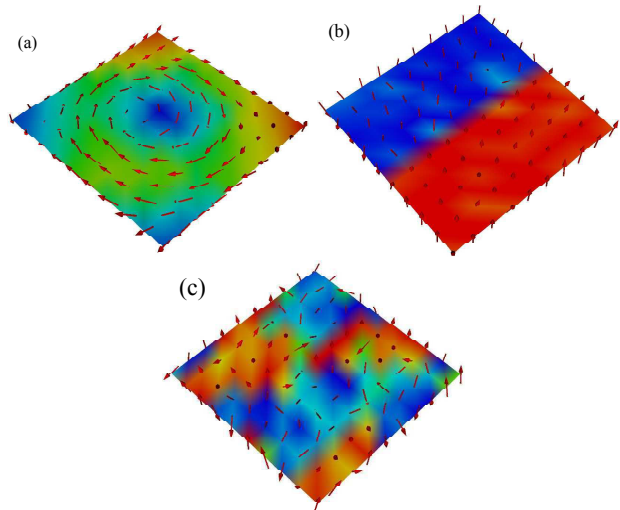


Figure 7. (Color online) Snapshots of the dot at (a) $T = 0.01$, (b) $T = 0.19$, (c) $T = 0.82$, for $A/D = 1.4/0.3 \simeq 4.6$, $L = 10$. The same color codes as in Fig. 1 are used.

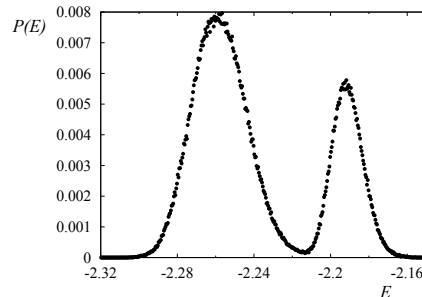


Figure 8. Energy histogram taken at the transition temperature $T_c = 0.111$ of the case $L = 10$ and $A/D = 1.4/0.3$.

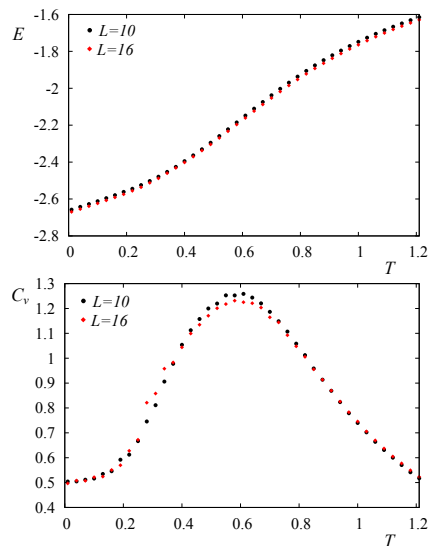


Figure 9. (Color online) Top: Energy per spin, Bottom: Specific heat, versus T for $A/D = 1.8/0.3 = 6$, with $L = 10$ (black circles) and $L = 16$ (red diamonds). See text for comments.

in Fig. 3. From the determined GS's, we have studied finite-temperature behaviors of nanodots. We found that for small A/D , there exists a second-order transition from the in-plane vortex ordering to the disordered phase: the peak of the specific heat as well as that of the susceptibility strongly depend on the system size. For larger A/D , there is a first-order re-orientation transition from in-plane to perpendicular ordering with a large latent heat. To our knowledge, such a transition in a very small system has never been observed before at a finite temperature. For much larger A/D , there is no phase transition. These results show that the core vor-

tex structure is stabilized at finite temperatures, making possible applications using perpendicular magnetization reversal^{8,11,12}.

ACKNOWLEDGEMENTS

This work was supported by the Polish National Science Centre (NCN) through the project UMO-2013/08/M/ST3/00967.

-
- ¹ H. T. Diep (ed.), *Frustrated Spin Systems*, 2nd edition, World Scientific, Singapore (2013).
- ² H. T. Diep, V. Bocchetti, Danh-Tai Hoang and V. T. Ngo, *Theory and Simulation of Magnetic Materials: Physics at Phase Frontiers*, <http://arxiv.org/abs/1309.4754> (2013).
- ³ A. Zangwill, *Physics at Surfaces*, Cambridge University Press, London (1988).
- ⁴ J.A.C. Bland and B. Heinrich (editors), *Ultrathin Magnetic Structures*, vol. I and II, Springer-Verlag, Berlin (1994).
- ⁵ C. Santamaria and H. T. Diep, *J. Mag. Mag. Mater.* **212**, 23 (2000).
- ⁶ D.-T. Hoang, M. Kasperski, H. Puzkarski and H. T. Diep, *J. Phys.: Cond. Matter* **25**, 056006 (2013).
- ⁷ C. S. Rocha, P. Z. Coura, S. A. Leonel, R. A. Dias and B. V. Costa, *J. Appl. Phys.* **107**, 053903 (2010).
- ⁸ T. Shinjo, T. Okuno, R. Hassdorf, K. Shigeto and T. Ono, *Science* **289**, 5481, 930-932 (2000).
- ⁹ J. Raabe, R. Pulwey, R. Sattler, T. Schweinbck, J. Zweck and D. Weiss, *J. Appl. Phys.* **88**, 4437 (2000).
- ¹⁰ A. Wachowiak, J. Wiebe, M. Bode, O. Pietzsch, M. Morgenstern and R. Wiesendanger, *Science* **298**, 18, 577-580 (2002).
- ¹¹ Q. F. Xiao, J. Rudge, E. Girgis, J. Kolthammer, and B. C. Choi, Y. K. Hong and G. W. Donohoe, *J. Appl. Phys.* **102**, 103904 (2007).
- ¹² N. Kikuchi, S. Okamoto, O. Kitakami, Y. Shimada, S. G. Kim, Y. Otani and F. Fukamichi, *J. Appl. Phys.* **90**, 6548 (2001).
- ¹³ F. J. A. den Broeder, D. Kuiper, A. P. van de Mosselaer and W. Hoving, *Phys. Rev. Lett.* **60**, 2769 (1988).
- ¹⁴ H. Kurt, M. Venkatesan and J. M. D. Coey, *J. Appl. Phys.* **108**, 073916 (2010).
- ¹⁵ Y. Hodumi, J. Shi and Y. Nakamura, *Appl. Phys. Lett.* **90**, 212506 (2007).
- ¹⁶ D. P. Landau and K. Binder, *A Guide to Monte Carlo Simulations in Statistical Physics*, Cambridge University Press, London (2009).
- ¹⁷ S. Brooks, A. Gelman, G. L. Jones and Xiao-Li Meng, *Handbook of Markov Chain Monte Carlo*, CRC Press (2011).
- ¹⁸ E. Yu. Vedmedenko, A. Ghazali and J.-C. S. Lévy, *Phys. Rev. B* **59**, 3329 (1999).
- ¹⁹ U. Nowak, R. W. Chantrell and E. C. Kennedy, *Phys. Rev. Lett.* **84**, 163 (2000).
- ²⁰ V. T. Ngo and H. T. Diep, *Phys. Rev. B* **75**, 035412 (2007).
- ²¹ G. M. Wysin, *Phys. Rev. B* **49**, 15156-15162 (1996).
- ²² M. E. Gouvêa, G. M. Wysin, A. R. Bishop and F. G. Martens, *Phys. Rev. B* **39**, 11840 (1989).
- ²³ J. Zinn-Justin, *Quantum Field Theory and Critical Phenomena*, 4th ed., Oxford Univ. Press (2002).
- ²⁴ D. J. Amit, *Field Theory, the Renormalization Group and Critical Phenomena*, World Scientific, Singapore (1984).
- ²⁵ N. D. Mermin and H. Wagner, *Phys. Rev. Lett.* **17**, 1133 (1966).
- ²⁶ V. Privman (ed.), *Finite-Size Scaling and Numerical Simulation of Statistical Systems*, World Scientific, Singapore (1998).
- ²⁷ H. T. Diep, *Theory of Magnetism - Application to Surface Physics*, World Scientific, Singapore, in press (2013).